Polymer Degradation and Stability 206 (2022) 110195

Contents lists available at ScienceDirect

Polymer Degradation and Stability

journal homepage: www.journals.elsevier.com/polymer-degradation-and-stability

Toward a deep understanding of the difference between isotactic and syndiotactic polypropylene on the fire performance and degradation behavior

Zhishuo Liu [a], Jinxuan Chen [a,b,c], Yifang Hua [a,b,c], Lijun Qian [b], Jun Sun [a,c,*], Hongfei Li [a], Xiaoyu Gu [a], Sheng Zhang [a,c,**]

[a] State Key Laboratory of Organic-Inorganic Composites, Beijing University of Chemical Technology, 100029, China
[b] Engineering Laboratory of Non-halogen Flame Retardants for Polymers, Beijing Technology and Business University, Beijing, 100048, China
[c] Beijing Key Laboratory of Advanced Functional Polymer Composites, Beijing University of Chemical Technology, Beijing, 100029, China

ARTICLE INFO

Keywords:
Isotactic polypropylene (iPP)
Syndiotactic polypropylene (sPP)
Flame retardant
Degradation behavior

ABSTRACT

This work investigated the difference in flame retardancy and degradation behavior of polypropylene (PP) composites with different configurations. The piperazine pyrophosphate (PAPP) was combined with melamine polyphosphate (MPP) to construct an intumescent flame retardant system, before incorporating into the PP system by melt blending. It showed that by the introduction of equal amounts of flame retardant, isotactic polypropylene composites (iPP-IFR) can achieve better flame retardancy with a desirable UL-94 V-0 rating, whereas syndiotactic polypropylene (sPP-IFR) shows poor fire performance. Melt index tests show that sPP-IFR sample is easy to flow and prone to melt drops. Differential scanning calorimetry results show that iPP-IFR has a higher degree of crystallinity. The thermogravimetric infrared coupling results show that sPP-IFR produces more small molecule hydrocarbon gases during combustion, making the system more difficult to achieve satisfied flame retardancy. The burning properties of iPP-IFR have been proven to be somewhat better compared to that of sPP-IFR, and sPP is more difficult for flame retardant modification.

1. Introduction

Polypropylene (PP) is a commonly used thermoplastic resin [1]. PP has been widely used in many industries such as automotive, chemical and constructional fields because of its abundant sources, light weight, corrosion resistance, low price and good mechanical properties [2–4]. PP can be divided into isotactic polypropylene (iPP), syndiotactic polypropylene (sPP) and atactic polypropylene (aPP) according to the distribution of its branched atoms on both sides of the main chain, and the specific structure is shown in Fig. 1 [5]. iPP endows good crystallinity, melting point, tensile strength, flexural modulus, and impact strength due to its high regularity [6]. At present, commercial PP materials mostly use iPP as the matrix material. With the use of new catalysts in recent years, sPP with commercial applications have been synthesized. Different from iPP that exhibits typical plastic properties, sPP is a thermoplastic elastomer with relatively high modulus [7–9]. Compared to iPP, sPP is more ductile with higher impact strength, better toughness and transparency [10,11].

Since PP has no heteroatom on its molecular chain, it is highly flammable without char-forming ability. Once ignited, PP will release a large amount of heat quickly, accompanied by serious molten drops [12,13]. They can easily ignite other combustible materials and cause a large-scale fire, resulting in the restriction of applications in many fields. Therefore, the flame retardant modification of PP is of significance.

The commonly used flame retardants for PP are brominated flame retardants, inorganic flame retardants, phosphorus/nitrogen flame retardants and intumescent flame retardants (IFR), etc [14,15]. IFR is a compound flame retardant with nitrogen and phosphorus as the main components, and consists of an acid source, a char source, and a gas source, which can be regarded as an environmentally friendly flame retardant [16–18]. Yuan et al. prepared an efficient intumescent flame retardant (IFR) for flame retardant polypropylene using ammonium polyphosphate (APP) and polypiperazine phenyl phosphoramidite charcoal (BPOPA) as raw materials, and achieved good flame retardancy

* Corresponding author.
** Co-corresponding author.
E-mail addresses: sunj@mail.buct.edu.cn (J. Sun), zhangsheng@mail.buct.edu.cn (S. Zhang).

https://doi.org/10.1016/j.polymdegradstab.2022.110195
Received 6 October 2022; Received in revised form 6 November 2022; Accepted 7 November 2022
Available online 8 November 2022

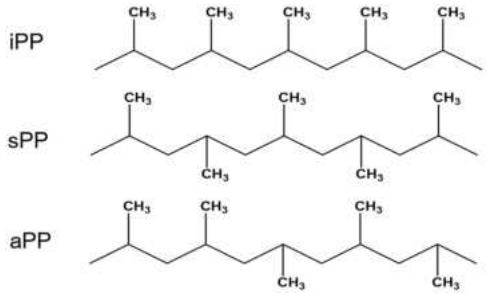

Fig. 1. Structure diagram of polypropylene with different structures.

Table 1
The experimental formulations.

Sample	Composition (wt%)			
	iPP	sPP	PAPP	MPP
Ipp	100	0	0	0
sPP	0	100	0	0
iPP-IFR	82	0	12.6	5.4
sPP-IFR	82	0	12.6	5.4

with V-0 rating at 25% loading [19]. In addition, MPP and pentaerythritol are also commonly used intumescent flame retardants for polypropylene [20]. Piperazine pyrophosphate (PAPP) is a new type of IFR with three components at the same time. Its excellent flame retardant characteristics are particularly suitable for polyolefin, especially for PP [21,22]. Hu et al. studied the effect of compounding piperazine pyrophosphate with melamine polyphosphate on the flame retardancy of PP, and found that the two have a better char formation effect [23].

There has been widespread research on the flame retardancy of iPP, but rare attention has been paid to sPP. iPP and sPP have different properties, such as melt index. Upon exposure to heat flow, PP melts first and produces molten droplets, which may lead to flame propagation. The dripping phenomenon is closely related to the melt viscosity. Moreover, both the forming process and the strength of the formed char layer are also affected by the melt viscosity [24,25]. The complete and dense char layer can effectively inhibit flammable volatiles escaping from the interiors and shield the underlying matrix from the exterior heat irradiation. [26–28] To the best of our knowledge, there is no report to study the difference in the fire performance for PP materials with different structures.

In this paper, PAPP is compounded with MPP to prepare a highly effective intumescent flame retardant system for PP. The limiting oxygen index (LOI), UL-94 vertical burning test and cone calorimetry test were performed to characterize the combustion properties of PP. More importantly, the differences of iPP and sPP on the combustion properties was investigated and the corresponding mechanism was proposed. This work provides an innovative perspective to study the correlation between the molecular structure of PP, combustion behavior, and flame retardancy mechanism. It is expected to provide theoretical guidance for the subsequent preparation of flame retardant PP composites.

2. Experiment

2.1. Material

Isotactic polypropylene (iPP, MI≈2.6 g/10min) was purchased from Maoming Petrochemical Co., Ltd. China. Syndiotactic polypropylene (sPP, MFI ≈ 3.5 g/10min) was purchased from TOTAL, France. Melamine polyphosphate (MPP) was purchased from Zhenjiang Star Flame Retardant Co., Ltd. Piperazine pyrophosphate (PAPP, Whiteness ≥95%) was purchased from Chongqing Kejufu New Material Co. Ltd. The above samples were used directly without any further purification.

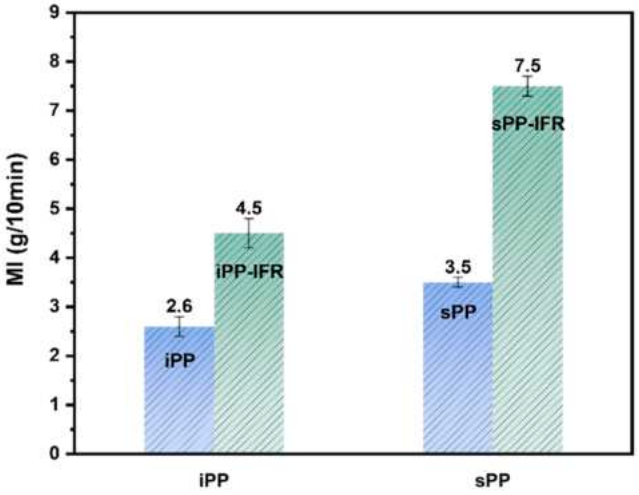

Fig. 2. Melting index of PP and its composites.

2.2. Preparation of iPP and sPP composites

The iPP and sPP composite samples were melt compounded at 180°C for 10 min with the rotate speed of 50 rpm using a torque rheometer (Harbin Harp Electric Technology Co., Ltd.). The iPP-IFR and sPP-IFR samples were then prepared by a micro injection molding machine at 220°C to obtain standard specimens with different sizes for subsequent testing. The formulations for the different PP samples are listed in Table 1.

2.3. Characterization

The melt index (MI) of all PP samples were measured by a melt flow indexer (MTS\SANS ZRZ1452, China) with a load of 2.16 kg at 210°C. The MI values were calculated according to the average of 5 parallel measurements.

The limiting oxygen index (LOI) was measured according to ISO 4589-2 using a JF-3 oxygen index meter (Jiangning District Instrument Factory, Nanjing, China) with the sample size of 100 × 6.5 × 3.2 mm^3. Five parallel samples were tested in each group to obtain an average.

The UL-94 vertical burning test (UL-94) was tested by the JF-3 horizontal vertical flame tester (Jiangning Analytical Instruments, China) according to ISO 9773 with a specimen size of 100 × 13 × 3.2 mm^3. Five parallel samples are tested in each group.

The cone calorimeter test (CONE) was carried out in a cone calorimeter (FTT) with a sample dimension of 100 × 100 × 3 mm^3. The test was under a heat flux density of 50 kW/m^2. The values were averaged from at least 3 parallel specimens.

The morphologies were observed by scanning electronic microscopy (SEM) on a HITACHI S4700 instrument at an accelerating voltage of 20 kV.

Thermogravimetric analysis (TGA) was performed in a TA-Q50 instrument under air or N_2 atmosphere. The specimen with around 5 mg was heated from ambient temperature to 800°C at a rate of 10°C/min.

DSC curves were recorded by using a TA Q-20 instrument under a N_2 atmosphere at a flow rate of 50 mL/min. Each specimen (about 5 mg) was heated from ambient temperature to 220°C at 10°C/min to eliminate heat history and then cooled to ambient temperature before being heated to 220°C at the same heating rate.

Thermogravimetric analyzer coupled with Fourier transform infrared spectrometer (TG-FTIR) testing of the samples was carried out to measure the volatiles during the thermal degradation of two PP composites using an FT-IR spectrophotometer (Nicolet) with a scanning range of 4000-500 cm^{-1} and a resolution of 1.0 cm^{-1} with 32 scans. Air was used as the carrier gas so that the gaseous product enters the IR gas

Table 2
The LOI and UL-94 rating of PP composites.

Samples	LOI (%)	UL-94 t_1/t_2 (s)	Dripping	Rating
iPP	18.5±0.5	45.0/-*	Y	NR
sPP	17.5±0.5	42.0/-*	Y	NR
iPP-IFR	30.8±0.5	0.2/4.8	N	V0
sPP-IFR	29.3±0.5	4.1/45	Y	NR

* The material burns completely.

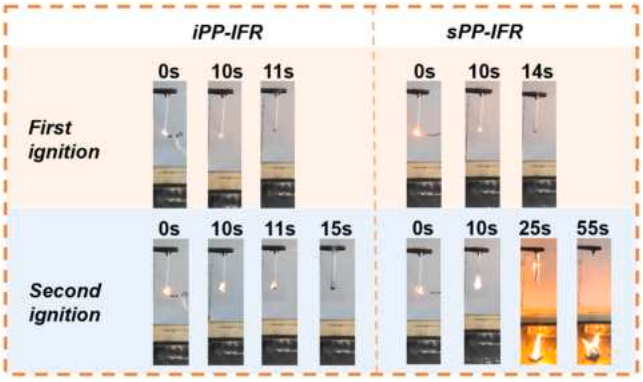

Fig. 3. Video snapshots of the vertical burning tests of PP composites.

chamber directly for FT-IR analysis. To avoid condensation of the released volatiles, the temperature of the gas chamber and transmission line was kept constant at 180°C.

3. Results and discussion

3.1. Melt Index Test

The MI of iPP, sPP, iPP-IFR and sPP-IFR is measured to investigate the effect of the molecular structure and the existence of IFR on the rheology property of the matrix, and the results are shown in Fig. 2. As can be seen in Fig. 2, the difference of MI between iPP and sPP is relatively small, which are 2.6 g/10min and 3.5 g/10min respectively. The MI of iPP-IFR is increased to 4.5 g/10min, and MI of sPP-IFR is significantly increased to 7.5 g/10min. It is suggested that the introduction of the IFR breaks the molecular chain of the matrix, leading to the increase of MI [29,30]. Compared to iPP, sPP has more random chain segments, which is attributed to the breakage of more molecular chains [31].

3.2. Flame retardancy

The flame retardant properties of PP are studied by UL-94 and LOI tests, and the corresponding data are shown in Table 2. The video snapshot of the UL-94 test for PP composites is shown in Fig. 3. It is clear that the LOI values for iPP and sPP are only 18.5% and 17.5%. They all fail in the UL-94 test and are accompanied with severe melt dripping during combustion. The addition of 12.6wt% PAPP and 5.4wt% MPP to the PP matrix can significantly increase the LOI value to 30.8% and 29.5% for iPP and sPP, respectively. However, the dripping phenomenon for sPP-IFR sample during the UL-94 test still exists, so the V-0 rating cannot be achieved. By comparison, with the same loading of IFR, the iPP-IFR composites can reach a desirable V-0 rating with no dripping produced. In view of the above performance, the introduction of IFR shows better flame retardant effect for iPP, compared to sPP.

In order to further evaluate the effect of flame retardant on iPP and sPP, cone calorimetry test is conducted, and the relevant data are shown

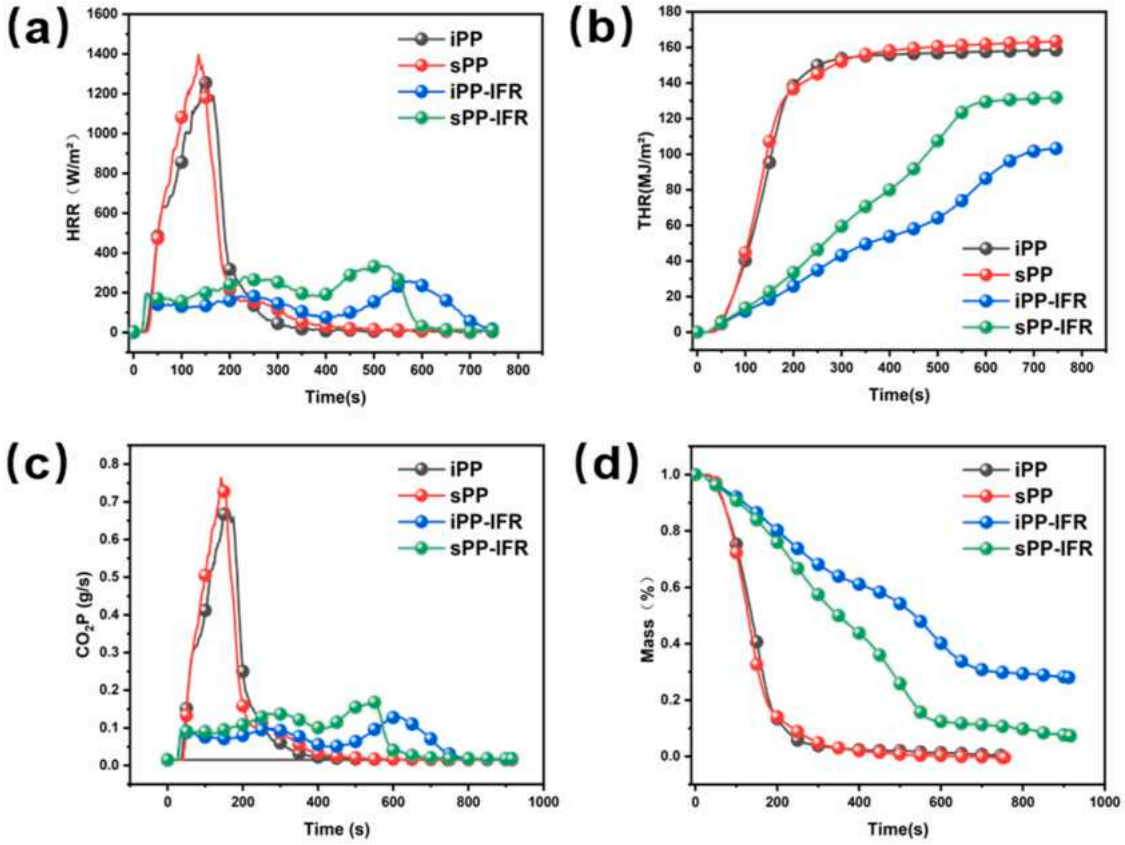

Fig. 4. HRR (a), THR (b), CO_2P(c) and Mass (d) curves for different PP samples.

Table 3
Cone calorimeter data of PP composites.

Samples	pHRR (kW/m^2)	THR (MJ/m^2)	CO_2P (g/s)	Mass (%)
iPP	1257±55	157±7	0.68±0.06	0.7±0.1
sPP	1397±56	163±5	0.76±0.09	0.04±0.01
iPP-IFR	257±24	102±5	0.12±0.02	28.61±0.9
sPP-IFR	335±25	132±6	0.17±0.03	7.89±0.6

in Fig. 4 and Table 3. The results of heat release rate (HRR), total heat release (THR), peak CO_2 release (CO_2P) and specimen mass for iPP, sPP, iPP-IFR and sPP-IFR are exhibited in Fig. 4. As shown in Fig. 4(a), it can be seen that both iPP and sPP burn very quickly after ignition. Among them, the peak heat release rate (pHRR) value of iPP is 1251.7 kW/m^2, while that of sPP is 1402.3 kW/m^2. The trend of THR is similar to that of HRR for iPP and sPP composites (shown in Fig. 4(b)). During combustion, the THR of iPP is 157.5 MJ/m^2 and the THR of sPP is higher than iPP at 162.5 MJ/m^2. sPP has a lower oxygen index and higher pHRR and THR values, indicating that sPP is more combustible than iPP. With the incorporation of IFR, the pHRR and THR values of iPP-IFR and sPP-IFR are significantly decreased. The pHRR and THR of sPP-IFR drop to 333.4 kW/m^2 and 131.5 MJ/m^2. In addition, the pHRR of iPP-IFR is decreased to 258.3 kW/m^2, much lower than that of sPP-IFR. At the same time, the THR value of sPP-IFR (132 MJ/m^2) is higher than that of iPP-IFR (101.8 MJ/m^2) during the combustion process. According to above results, it indicates that IFR has a more obvious improvement in the flame retardancy of the iPP matrix.

CO_2 production is not only important for assessing fire hazards, but also provides some objective evidence for fire retardant mechanisms. CO_2 is produced mainly from the full combustion of combustible materials and the significant reduction in CO_2 production is mainly due to the dilution of combustible materials in the gas phase and the barrier effect of the char layer in the solid phase during combustion [32, 33]. After adding the IFR, the release of CO_2 is significantly reduced. The CO_2 release from iPP-IFR and sPP-IFR is reduced to 0.12 g/s and 0.17 g/s, respectively. This indicates that the sPP-IFR sample burns more completely than iPP-IFR sample, and the Mass results can also indicate this conclusion.

3.3. Residue analysis

In order to gain insight into the way in which IFR acts in the condensed phase, the char residues of iPP, sPP, iPP-IFR and sPP-IFR samples are also investigated, and the external microstructure of the residues is further analyzed by SEM. As shown in Fig. 5, both iPP and sPP burn completely, leaving a negligible amount of char residue after combustion. It can be seen that all flame retardant PP samples leave a clear and large amount of char residue, which shows a protective effect on the underlying material.

The digital photographs of the two flame retardant PP samples show that the char layer of sPP-IFR is 0.3 cm higher than that of iPP-IFR. In SEM images, some obvious cracks and pores can be seen in the sPP-IFR composites, which means that the char layer cannot protect the matrix well from decomposition. In contrast, the char layer of iPP-IFR is flat and continuous, which can effectively block external oxygen and heat from entering the underlying PP substrate and achieving flame retardancy. It is evident that the IFR play an excellent role as a flame retardant in the condensed phase of the PP matrix.

During the combustion of the sample, the char source in the IFR undergoes an esterification reaction catalyzed by the acid source. With the increase of temperature, the gas source in the IFR leads to expanding and foaming. The char structure can be affected by the expanding process, and the MI is a key factor. sPP-IFR sample shows a high MI compared to iPP-IFR, and the sample has a better flow in the molten state. This may lead to the formation of char layer with more porous. It can be deduced that the loose porous char layer of sPP-IFR does not protect the sample very well. On the contrary, the MI of iPP-IFR sample is to the benefit of forming dense and continuous char layer, which can better protect the polymer and hinder the entry of combustible gas. This also explains the reason why iPP-IFR exhibits the lowest pHRR and THR values.

3.4. Thermal stability

The TG and DTG curves of iPP, sPP and their composites are showed in Fig. 6, and the corresponding characteristic data are showed in

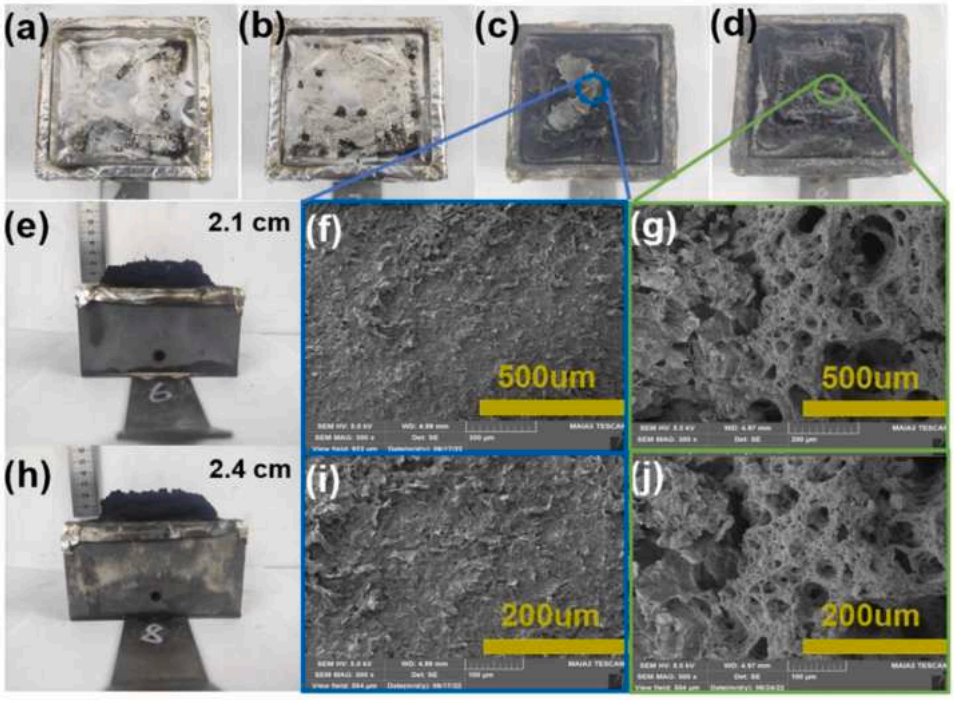

Fig. 5. Digital photos and external surface SEM images of the char residues after the CONE tests for iPP (a), sPP (b), iPP-IFR (c, e, f, i) and sPP-IFR (d, h, g, j).

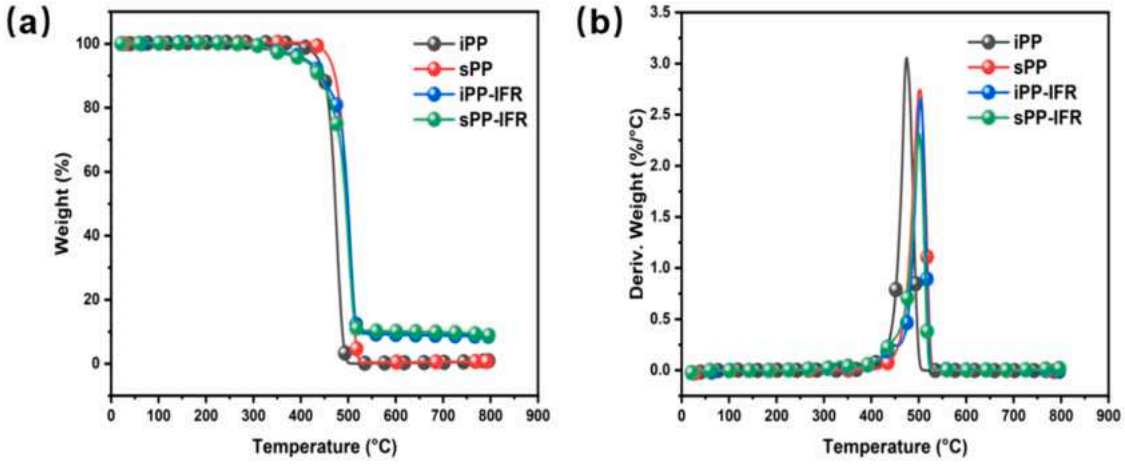

Fig. 6. TG (a) and DTG (b) curves of iPP, sPP, iPP-IFR and sPP-IFR under N_2 atmosphere.

Table 4
TG and DTG data of PP and its composites under N_2 atmosphere.

Sample	$T_{5\%}$ (°C)	T_{max} (°C)	Char yield at 700°C (wt%)
iPP	440	475	0.9
sPP	460	502	0.2
iPP-IFR	407	503	8.9
sPP-IFR	404	501	7.1

Table 5
Location of characteristic bands of gases released from PP.

Evolved gases	FTIR/cm^{-1}
Alkanes	2960,2915,1460,1380
Olefins	3080,1650,910
C=O	1670
NH_3	965,930
Phosphorous compounds	1085,853

Table 4, including the initial thermal decomposition temperature ($T_{5\%}$), the temperature corresponding to the maximum weight loss rate (T_{max}) and residual char at 700°C. It can be found in Fig. 6 (a) that there are similar one-step thermal degradation behaviors in iPP, sPP and its composites. Analysis of the $T_{5\%}$ shows that the $T_{5\%}$ of sPP-IFR and iPP-IFR samples are lower than the neat sample. This is due to the early decomposition of the flame retardant.

The residual char formation of iPP, sPP and their composites at 700°C is shown in Table 4. The amount of residual char is significantly higher for iPP-IFR and sPP-IFR relative to the control samples. iPP and sPP exhibit similar thermal degradation process. Both iPP and sPP exhibit a one-step decomposition in the range of 440-510 °C. The remaining 0.9% of charcoal in the iPP is higher than the sPP. At 700°C, the residual char of iPP-IFR (8.9%) is higher than that of sPP-IFR (7.1%). This suggests that IFR plays a role in promoting char formation and improving the thermal stability of PP, and the char formation effect is more obvious with IFR in iPP.

3.5. Gas-phase action analysis

TGA-FTIR is used to study the real-time evolution of gaseous products of iPP-IFR and sPP-IFR samples, in order to infer the differences in their thermal degradation properties. The locations of the characteristic bands are summarized in Table 5, and Fig. 7 shows the FT-IR spectra.

Under nitrogen atmosphere, hydrocarbons are identified as a decomposition product of both composites. In addition to hydrocarbons, they also release NH_3 and phosphorous compounds, mainly from the decomposition of MPP in the flame retardant system [34,35]. As a non-flammable gas, NH_3 not only expands the char layer, but also functions as a fuel diluent in the gas phase. This result is due to the fact that iPP and sPP have a fully aliphatic hydrocarbon structure. At the same time, both iPP-IFR and sPP-IFR samples release the same type of decomposition products.

Fig. 7 (b) and (c) depict the intensity of the characteristic absorption peaks of alkanes and olefins as a function of temperature. It is obvious that the intensity of the characteristic absorption peaks of alkanes and olefins of the sPP-IFR composite are stronger than those of the iPP-IFR composite. The hydrocarbons in the gas phase are mainly derived from the decomposition of PP [36,37]. The incomplete char layer leads to more sPP-IFR sample involved in combustion, releasing more combustible hydrocarbon gas material, promoting heat and oxygen transfer in the combustion cycle and reducing the flame retardant efficiency. That's why the LOI values of sPP are lower than those of iPP, which is consistent with the cone calorimetry test results.

The intensity of the characteristic peaks of NH_3 as a function of temperature is depicted in Fig. 7 (d), with the release of NH_3 showing two distinct phases. The first stage is attributed to the elimination of amino groups from the MPP and the second is attributed to the decomposition of nitrogenous compounds in the char layer [38]. Among the two composites, the NH_3 release from sPP-IFR is slightly higher than that from iPP-IFR. This is due to the fact that more sPP-IFR samples are involved in the combustion and therefore more nitrogenous compounds are decomposed in the char layer. The intensity of carbonyl groups generate from iPP-IFR and sPP-IFR decomposition under nitrogen atmosphere is shown in Fig. 7 (f). The peak intensity of the sPP-IFR carbonyl group is higher than that of iPP-IFR. This is probably due to the fact that sPP is catalyzed by the acidic flame retardant during processing and more molecular chain breaks occur, producing more carbonyl groups. At the same time this has led to a marked increase in MI.

3.6. DSC Testing

The DSC curves of iPP, sPP and their composites are shown in Fig. 8 and the relevant data are summarized in Table 6. In the DSC heating curve of iPP, an obvious melting point is found at 165.7°C, which is the typical α-form crystal. The crystallinity of the iPP reaches 43.8%. However, after the adding of 18wt% IFR, a new melting point appears at 150.2 °C, which is assigned to the melting of β-form crystal. The reason is that the IFR particles acted as the heterogeneous nucleating agent to induce the growth of β-form crystal [39,40]. On the other hand, the rigid IFR particles hinder the movement and regular arrangement of flexible PP molecular chains, the total crystallinity is reduced to 35.4%. In other

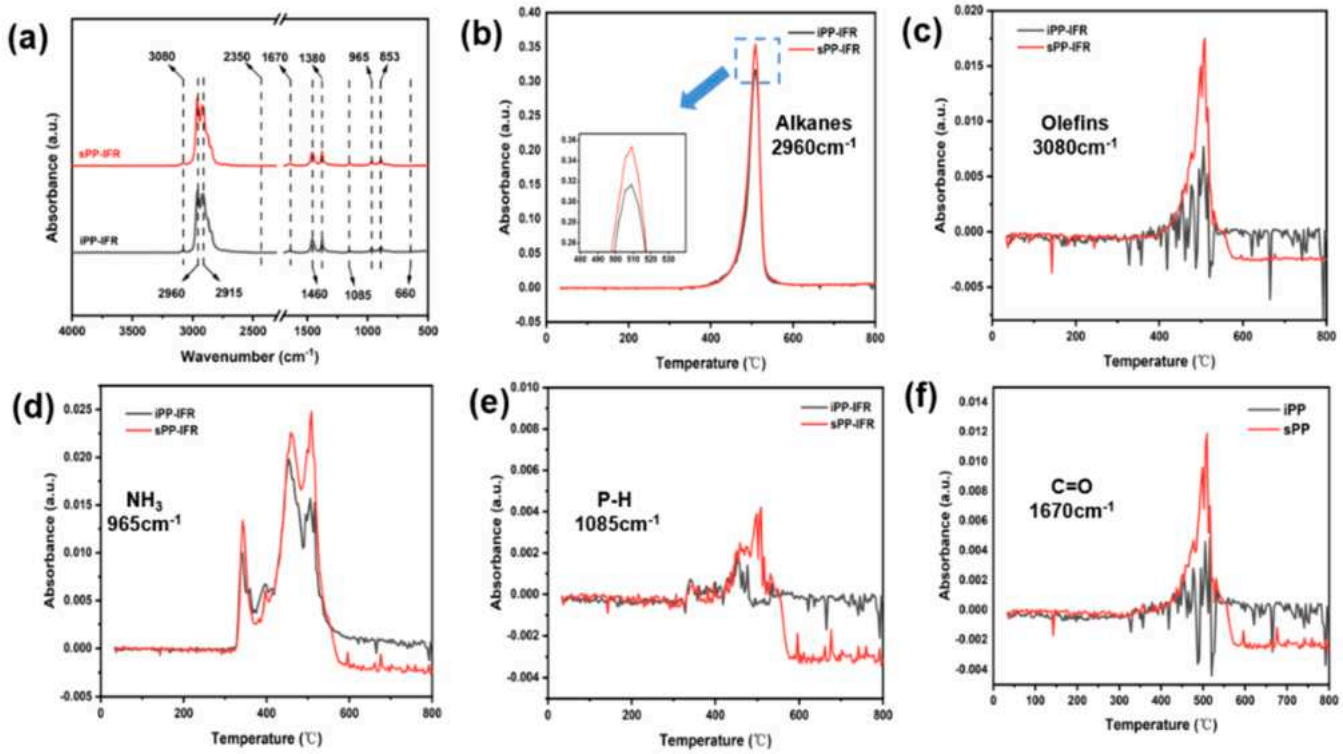

Fig. 7. Characteristic evolutionary gas spectra of flame retardant composites: (a); Characteristic peaks of the gas of interest with temperature: (b), (c), (d), (e) and (f).

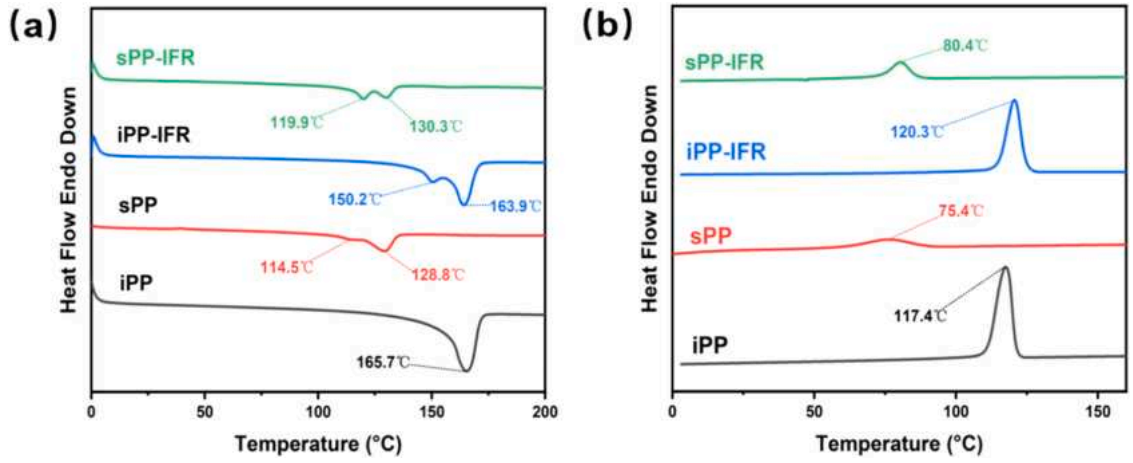

Fig. 8. DSC curve of sPP, iPP and their blends (a), heating curve, (b), cooling curve.

Table 6
DSC and crystallization data of PP and its composites.

Sample	T_m (°C)	T_c (°C)	ΔH_m (J/g)	ΔH_c (J/g)	Crystallinity (%)	ΔCrystallinity (%)
iPP	165.5	117.4	90.6	90.2	43.8	
sPP	114.5/ 129.4	75.4	25.7	23.9	29.3	
iPP-IFR	150.2/ 163.9	120.3	73.2	70.6	35.4	19.2
sPP-IFR	119.9/ 130.3	80.4	18.5	17.3	21.0	28.3

words, the amorphous percentage is increased in the whole system.

During the cooling process, the crystallization peak is appeared at 117.4 °C, and the IFR particles induce earlier crystallization of iPP. Therefore, the crystallization peak moves a little ahead to 120.3 °C, but the crystallinity of iPP is still higher than that of iPP-IFR.

For the sPP, its melting temperature is much lower than that of iPP. During the heating process, two melting points can be found at 114.5 and 129.4 °C. The crystallinity of sPP is only 29.3%. After adding 18wt% IFR, the melting point increase a little to 119.9 °C and 130.3 °C, but still much lower than that of iPP-IFR. The crystallinity is decreased to 21.0%. In this sense, the influence of IFR on the crystallization of sPP is significant. Meanwhile, the crystallinity of sPP-IFR is much lower than that of iPP-IFR.

During cooling, the crystallization of solo sPP is slow, the whole crystallization is finished from 90 °C to 61 °C, and the peak temperature is 75.4 °C. However, the crystallization speeds up for the sPP-IFR, and the crystallization scope is shortened in 70-90 °C. For the IFR particles that act as heterogeneous nucleating agent, the peak moves ahead to

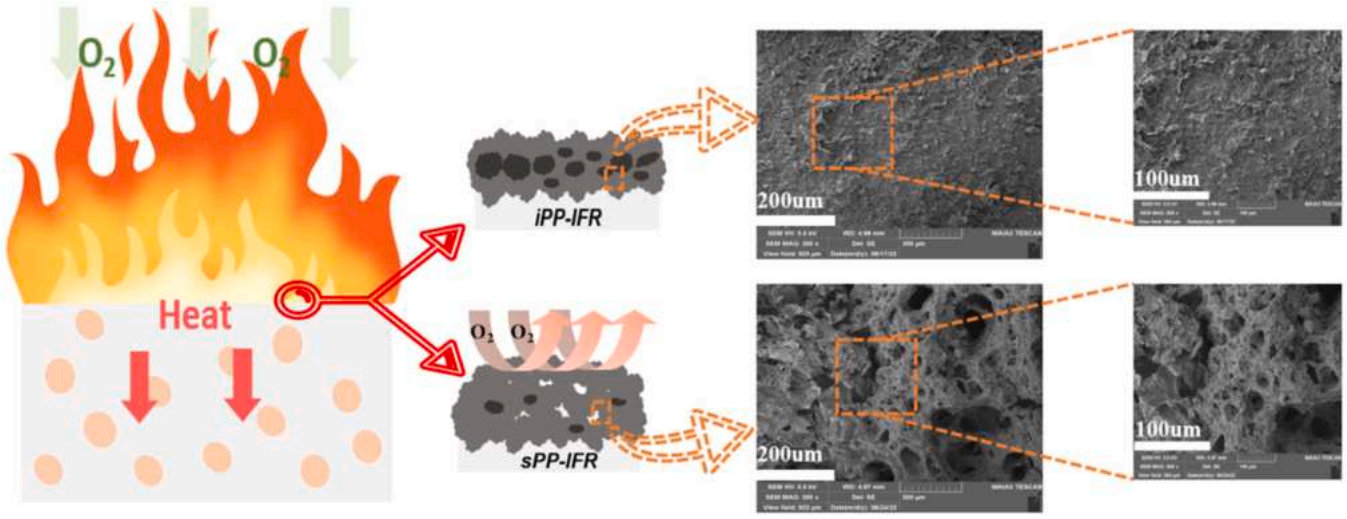

Fig. 9. The possible combustion mechanisms.

80.4 °C.

Compared to iPP-IFR, sPP-IFR has a lower melting temperature and crystallinity. During the heating process, sPP-IFR undergoes a more complete molecular chain movement at lower temperatures, making it easier for the material to develop molten droplets during combustion and more difficult to form a complete and dense char layer.

3.7. Combustion mechanism

The combustion mechanism is simulated in Fig. 9. In summary, iPP and sPP exhibit different combustion properties and ease of flame retardancy. During flame combustion, the random molecular chain segments in the sample are heated first and are more susceptible to movement and molecular chain breakage. Samples with a high MI affect the effect of the gas source in the IFR, causing the sample to expand and foam incompletely, affecting the quality of the resulting char layer, and also making it more likely to produce molten droplets in the UL-94 test [41]. The melting point and crystallinity of sPP-IFR are lower than those of iPP-IFR. sPP-IFR undergoes a more complete molecular chain movement at a lower temperature, obtaining better mobility. Due to the high MI of sPP-IFR, the integrity of foamed char is poor, with more pore structure and more break formed. As the flame burns, the small molecules produced by the matrix tend to contact with the flame, destroying the char layer formed by the flame retardant and eventually causing the flame to burn further [42]. iPP-IFR has a high crystallinity, melting point and a low MI. The strength of the melt is better at the initial stage of combustion, allowing a denser char layer to be formed. As a result, the small molecules produce by combustion can be isolated by the char layer inside the matrix and cannot contact with the external flame directly, effectively blocking heat and combustible gases, thus providing better flame retardancy [43].

4. Conclusion

In this work, PAPP and MPP (7:3) were mixed to form an intumescent flame retardant system and added to PP with different configurations to explore the effect of molecular structure on the combustion and flame retardant behavior. With the same IFR addition, iPP-IFR showed better flame retardancy, obtained a UL-94 V-0 rate and an LOI value of 30.8%, while the LOI of sPP-IFR was 29.3% and couldn't pass the UL-94 test. Meanwhile, iPP-IFR exhibited lower pHRR, THR and TSP and relatively higher residual char quality. According to the analysis, iPP-IFR had a greater proportion of crystalline areas, with higher melting point and lower MI compared to sPP-IFR. The sPP melt showed greater fluidity as well as lower strength, resulting in an unstable foaming structure that cannot be formed by the gas source of the IFR. Therefore, sPP-IFR was unable to formed a denser char layer. As a result, molten droplets and more combustible small molecules were produced during the combustion process. This impaired its flame retardant effect. In summary, the subsequent flame retardant modification of sPP should be carried out using a system with a significant charring and gas source. This enhances the protection of the substrate and dilutes the combustion gases generated by decomposition, thus effectively inhibiting the continuation of combustion. This work provides new ideas for exploring the mechanism of polymer combustion and has constructive guidance for preparing high-efficiency flame-retardant polyolefin composites.

CRediT authorship contribution statement

Zhishuo Liu: Conceptualization, Data curation, Formal analysis, Investigation, Methodology, Writing – original draft. **Jinxuan Chen:** Investigation, Methodology. **Yifang Hua:** Methodology. **Lijun Qian:** Methodology. **Jun Sun:** Resources, Supervision. **Hongfei Li:** Resources, Supervision. **Xiaoyu Gu:** Resources, Supervision. **Sheng Zhang:** Funding acquisition, Conceptualization, Resources, Supervision, Writing – review & editing.

Declaration of Competing Interest

The authors declare that they have no known competing financial interests or personal relationships that could have appeared to influence the work reported in this paper.

Data Availability

Data will be made available on request.

Acknowledgments

The authors would like to thank the National Natural Science Foundation of China (No.22175017 and No.22075010) and the Open Project Program of Engineering Laboratory of Non halogen Flame Retardants for Polymers, Beijing Technology and Business University, China (BTBUFR22-1) for their financial support of this research.

References

[1] X Zhu, Y Chen, C Zang, Flame retardant properties and mechanical properties of polypropylene with halogen and halogen-free flame retardant system, J. Phys. Conf. Ser. 2160 (2022) 012–031.

[2] Y Yuan, B Yu, W Wang, The influence of poorly-/well-dispersed organo-montmorillonite on interfacial compatibility, fire retardancy and smoke suppression of polypropylene/intumescent flame retardant composite system, J. Colloid Interface Sci. 622 (2022) 367–377.

[3] SH Wang, JS Li, WJ Wang, XG Wang, HF Li, J Sun, et al., Silicone filled halloysite nanotubes for polypropylene composites: Flame retardancy, smoke suppression and mechanical property, Composites Part A 140 (2021) 11.

[4] WF Tang, LX Song, F Liu, W Dessie, ZD Qin, S Zhang, et al., Improving the flame retardancy and thermal stability of polypropylene composites via introducing glycine intercalated kaolinite compounds, Appl. Clay Sci. 217 (2022) 10.

[5] A Eckstein, J Suhm, C Friedrich, RD Maier, R Mülhaupt, Determination of plateau moduli and entanglement molecular weights of isotactic, syndiotactic, and atactic polypropylenes synthesized with metallocene catalysts, Macromolecules 31 (1998) 1335–1340.

[6] A Rg, A Ha, B Ik, C Nm, C Mb, B Ra, On the effective elastic properties of isotactic polypropylene, Polymer 160 (2019) 291–302.

[7] R Odda, CD Rosa, F Auriemma, RD Girolamo, M Scoti, Thermoplastic elastomers from binary blends of syndiotactic polypropylenes with different stereoregularity, Polymer 85 (2016) 114–124.

[8] O Ballesteros, FD Stefano, F Auriemma, RD Girolamo, CD Rosa, Evidence of nodular morphology in syndiotactic polypropylene from the quenched state, Macromolecules 54 (2021) 7540–7551.

[9] RF Auriemma, Structure and physical properties of syndiotactic polypropylene: A highly crystalline thermoplastic elastomer, Prog. Polym. Sci. 31 (2006) 145–237.

[10] X Wang, J Yi, L Wang, Y Yuan, J Feng, Thermorheological evidence and structure of heterogeneity in syndiotactic polypropylene melts with strong memory effects, Polymer 218 (2021), 123484.

[11] B Dang, J He, J Hu, Z Yao, Tailored sPP/Silica Nanocomposite for Ecofriendly Insulation of Extruded HVDC Cable, J. Nanomater. 16 (2015) 439.

[12] R Ying, D Yuan, W Li, X Cai, Flame retardant efficiency of KH-550 modified urea-formaldehyde resin cooperating with ammonium polyphosphate on polypropylene, Polym. Degrad. Stab. 151 (2018) 160–171.

[13] X Bo, B Lsa, B Jwa, B Yla, B Lqa, Enhancement of the intumescent flame retardant efficiency in polypropylene by synergistic charring effect of a hypophosphite/cyclotetrasiloxane bi-group compound, Polym. Degrad. Stab. 181 (2020), 109281.

[14] B Wza, B Ckka, B Zla, B Xla, B Zza, Flame retardant treatments for polypropylene: Strategies and recent advances, Composites Part A: Appl. Sci. Manuf. 145 (2021), 106382.

[15] W Tang, L Qian, Y Chen, Y Qiu, B Xu, Intumescent flame retardant behavior of charring agents with different aggregation of piperazine/triazine groups in polypropylene, Polym. Degrad. Stab. 169 (2019), 108982.

[16] WX Li, HJ Zhang, XP Hu, WX Yang, CQ Xie, Highly Efficient Replacement of Traditional Intumescent Flame Retardants in Polypropylene by Manganese Ions Doped Melamine Phytate Nanosheets, J. Hazard. Mater. 398 (2020), 123001.

[17] Chao Guoxing, Juan, Flame retardant effect of cytosine pyrophosphate and pentaerythritol on polypropylene, Composites Part B 180 (2020), 107520.

[18] B Chen, W Gao, J Shen, S Guo, The multilayered distribution of intumescent flame retardants and its influence on the fire and mechanical properties of polypropylene, Compos. Sci. Technol. 93 (2014) 54–60.

[19] J Yuan, H Wang, Y Wang, Y Ma, Z Zhu, X Lin, A novel highly efficient intumescent flame-retardant polypropylene: Thermal degradation, flame retardance and mechanism, J. Polym. Res. 29 (2022) 1–10.

[20] Li Liping, Wang Gang, Guo Chuigen, Influence of intumescent flame retardant on thermal and flame retardancy of eutectic mixed paraffin/polypropylene form-stable phase change materials, Appl. Energy 162 (2016) 428–434.

[21] YA Zha, WB Hui, LA Yuan, WA Qi, Synergistic effect between piperazine pyrophosphate and melamine polyphosphate in flame retarded glass fiber reinforced polypropylene, Polym. Degrad. Stab. 184 (2021), 109477.

[22] S Lee, AB Morgan, DA Schiraldi, J Maia, Improving the flame retardancy of polypropylene foam with piperazine pyrophosphate via multilayering coextrusion of film/foam composites, J. Appl. Polym. Sci. 137 (2019) 48552.

[23] Z Hu, ZQ Zhong, XD Gong, Flame retardancy, thermal properties, and combustion behaviors of intumescent flame-retardant polypropylene containing (poly) piperazine pyrophosphate and melamine polyphosphate, Polym. Adv. Technol. 145 (2020) 4996.

[24] Yueming Yu, Liangdong Xi, Miaohong Yao, Linghui Liu, Yan Zhang, Siqi Huo, Zhengping Fang, Pingan Song, Governing effects of melt viscosity on fire performances of polylactide and its fire-retardant systems[J], iScience 25 (2022), 103950.

[25] X Wang, EN Kalali, DY. Wang, Renewable cardanol-based surfactant modified layered double hydroxide as a flame retardant for epoxy resin(Article)[J], ACS Sustainable Chem. Eng. 3 (2015) 3281–3290.

[26] Idumah Christopher Igwe, Hassan Azman, Bourbigot Serge, Synergistic effect of exfoliated graphene nanoplatelets and non-halogen flame retardants on flame retardancy and thermal properties of kenaf flour-PP nanocomposites(Article)[J], J. Thermal Anal. Calor. 134 (2018) 1681–1703.

[27] MF Liu, X Zhang, M Zammarano, JW Gilman, RD Davis, T. Kashiwagi, Effect of montmorillonite dispersion on flammability properties of poly(styrene-co-acrylonitrile) nanocomposites[J], Polymer 52 (2011) 3092–3103.

[28] Wen Xin, Min Jiakang, Tan Haiying, Gao Doudou, Chen Xuecheng, Szymańska Karolina, Zielińska Beata, Mijowska Ewa, Tang Tao, Reactive construction of catalytic carbonization system in PP/C60/Ni(OH)2 nanocomposites for simultaneously improving thermal stability, flame retardancy and mechanical properties.[J], Composites: Part A, Appl. Sci. Manuf. 129 (2020), 105722.

[29] Y Li, B Xue, S Wang, J Sun, S Zhang, The photoaging and fire performance of polypropylene containing melamine phosphate, ACS Appl. Polym. Mater. 2 (2020) 4455–4463.

[30] Sinturel Christophe, Philippart Jean-Louis, et al., Photooxidation of fire retarded polypropylene. I. Photoageing in accelerated conditions, Eur. Polym. J. 35 (1999) 1773–1781.

[31] Claudio De Rosa, Finizia Auriemma, Valeria Vinti, Maurizio Galimberti, Equilibrium melting temperature of syndiotactic polypropylene[J], Macromolecules 31 (1998) 6206–6210.

[32] SE Zhu, LL Wang, H Chen, W Yang, A Yuen, T Chen, et al., Comparative studies on thermal, mechanical, and flame retardant properties of pbt nanocomposites with functionalized amino-carbon nanotubes modified by different oxidation state phosphorus-containing agents, Nanomaterials-Basel 8 (2018) 70.

[33] A Zh, B Zwa, Synthesis of a copper hydroxystannate modified graphene oxide nanohybrid and its high performance in flexible polyvinyl chloride with simultaneously improved flame retardancy, smoke suppression and mechanical properties, Polym. Degrad. Stab. 183 (2020), 109425.

[34] M Nowak, B Cichy, E Kużdżał, Kinetics of melamine phosphate thermal decomposition in DSC studies, J. Therm. Anal. Calorim. 126 (2016) 277–285.

[35] Y Li, B Xue, S Wang, J Sun, S Zhang, The photoaging and fire performance of polypropylene containing melamine phosphate, ACS Appl. Polym. Mater. 2 (2020) 4455–4463.

[36] Z Qin, D Li, R Yang, Study on inorganic modified ammonium polyphosphate with precipitation method and its effect in flame retardant polypropylene, Polym. Degrad. Stab. 126 (2016) 117–124.

[37] L Qian, L Ye, Y Qiu, S Qu, Thermal degradation behavior of the compound containing phosphaphenanthrene and phosphazene groups and its flame retardant mechanism on epoxy resin, Polymer 52 (2011) 5486–5493.

[38] YA Zha, WB Hui, LA Yuan, WA Qi, Synergistic effect between piperazine pyrophosphate and melamine polyphosphate in flame retarded glass fiber reinforced polypropylene, Polym. Degrad. Stab. 184 (2020), 109477.

[39] MP Howard, ST Milner, A Simple Model for Heterogeneous Nucleation of Isotactic Polypropylene, Macromolecules 46 (2013) 32002.

[40] Heterogeneous Nucleation and Self-Nucleation of Isotactic Polypropylene Microdroplets in Immiscible Blends: From Nucleation to Growth-Dominated Crystallization, Macromolecules 53 (2020) 5980–5991.

[41] Y Wang, WD Kang, XY Zhang, F; Zhang, SX. Li, Development of a pendant experiment using melt indexer for correlation with the large-size dripping in the UL-94 test[J], Fire and Mater. 42 (2018) 436–446.

[42] CJ Zhu, MS He, Y Liu, JG Cui, QL Tai, L Song, Y. Hu, Synthesis and application of a mono-component intumescent flame retardant for polypropylene[J], Polym. Degrad. Stab. 151 (2018) 144–151.

[43] S Zhou, L Song, ZZ Wang, Y Hu, WY. Xing, Flame retardation and char formation mechanism of intumescent flame retarded polypropylene composites containing melamine phosphate and pentaerythritol phosphate.[J], Polym. Degrad. Stab. 93 (2008) 1799–1806.